In Vivo Evaluation of ^{11}C-DASB for Quantitative SERT Imaging in Rats and Mice

Michael Walker, Walter Ehrlichmann, Anke Stahlschmidt, Bernd J. Pichler, and Kristina Fischer

Department of Preclinical Imaging and Radiopharmacy, Werner Siemens Imaging Center, Eberhard Karls University of Tübingen, Tübingen, Germany

Serotonin, or 5-hydroxytryptamine (5-HT), plays a key role in the central nervous system and is involved in many essential neurologic processes such as mood, social behavior, and sleep. The serotonin transporter ligand ^{11}C-3-amino-4(2-dimethylaminomethyl-phenylsufanyl)-benzonitrile (^{11}C-DASB) has been used to determine nondisplaceable binding potential (BP_{ND}), which is defined as the quotient of the available receptor density (B_{avail}) and the apparent equilibrium dissociation rate constant ($1/appK_D$) under in vivo conditions. Because of the increasing number of animal models of human diseases, there is a pressing need to evaluate the applicability of ^{11}C-DASB to rats and mice. Here, we assessed the feasibility of using ^{11}C-DASB for quantification of serotonin transporter (SERT) density and affinity in vivo in rats and mice. **Methods:** Rats and mice underwent 4 PET scans with increasing doses of the unlabeled ligand to calculate B_{avail} and $appK_D$ using the multiple-ligand concentration transporter assay. An additional PET scan was performed to calculate test–retest reproducibility and reliability. BP_{ND} was calculated using the simplified reference tissue model, and the results for different reference regions were compared. **Results:** Displaceable binding of ^{11}C-DASB was found in all brain regions of both rats and mice, with the highest binding being in the thalamus and the lowest in the cerebellum. In rats, displaceable binding was largely reduced in the cerebellar cortex, which in mice was spatially indistinguishable from cerebellar white matter. Use of the cerebellum with fully saturated binding sites as the reference region did not lead to reliable results. Test–retest reproducibility in the thalamus was more than 90% in both mice and rats. In rats, B_{avail}, $appK_D$, and ED_{50} were 3.9 ± 0.4 pmol/mL, 2.2 ± 0.4 nM, and 12.0 ± 2.6 nmol/kg, respectively, whereas analysis of the mouse measurements resulted in inaccurate fits due to the high injected tracer mass. **Conclusion:** Our data showed that in rats, ^{11}C-DASB can be used to quantify SERT density with good reproducibility. BP_{ND} agreed with the distribution of SERT in the rat brain. It remains difficult to estimate quantitative parameters accurately from mouse measurements because of the high injected tracer mass and underestimation of the binding parameters due to high displaceable binding in the reference region.

Key Words: SERT; [^{11}C]DASB; B_{avail}; K_D; PET

Serotonergic neurons accumulate mainly in the brainstem and form the raphe nuclei (*1*). Although the raphe nuclei consist of only a few neurons, these nuclei innervate nearly all brain regions (*1*). Under normal physiologic conditions, the membrane-bound, sodium-chloride–dependent SERT (serotonin transporter, or 5-hydroxytryptamine [5-HT] transporter) is responsible for specific reuptake of released serotonin by cells (*2*). This transporter is located on the soma, dendritic collaterals, and entire axon of serotonergic neurons (*3*).

One of the most promising noninvasive imaging approaches for visualizing the distribution of SERT is the SERT marker ^{11}C-3-amino-4(2-dimethylaminomethyl-phenylsufanyl)-benzonitrile (^{11}C-DASB), which is designed for PET (*4*). This tracer has previously been used in pharmaceutical and clinical human PET studies as a high-affinity and highly selective radioligand for SERT (*4,5*).

However, ^{11}C-DASB has not been evaluated for in vivo PET experiments in mice. With the increasing number of transgenic animal models of human diseases and the availability of dedicated small-animal PET imaging systems, there is a pressing need for in vivo evaluation and quantification of this PET tracer (*6*). Because of the small size of rodent brain structures, a PET scanner with high spatial resolution and detection sensitivity is needed. In addition, if the injected tracer mass is greater than 1%–5% receptor occupancy in the region of interest, the measurement may violate the tracer principle and result in imprecise quantification (*7*).

For absolute tracer quantification and pharmacokinetic modeling, determination of the arterial input function or application of a reference tissue that does not show specific tracer binding is mandatory (*8*). Especially in small-animal longitudinal studies that require more than one PET scan of the same animal, application of an arterial input function through collection of blood samples is not practical. Therefore, we tested the applicability of different reference tissues and used the simplified reference tissue model to determine the nondisplaceable binding potential (BP_{ND}) in rats and mice (*9*).

In general, small animals need to be anesthetized during in vivo PET measurements. Thus, the effects of individual anesthetics on the pharmacokinetics of the radioligand and on its response to pharmacologic challenges play an important role for the interpretation of PET data (*10,11*). According to the literature, isoflurane can have a substantial impact on the behavior of SERT and may change the binding characteristics of the transporter to its ligand (*12*). Therefore, we tested two different anesthetics to evaluate their possible confounding effects on tracer uptake and binding behavior. BP_{ND} is defined as the quotient of the available receptor density (B_{avail}) and the apparent equilibrium dissociation rate constant

(1/appK_D). A change in BP_{ND} can therefore result from an alteration of B_{avail} or 1/appK_D. To estimate the B_{avail} and 1/appK_D of SERT separately, we used the multiple-ligand concentration transporter assay at pseudoequilibrium (13).

MATERIALS AND METHODS

Subjects

In this study, 8 male C57/BL6 mice (Charles River) and 4 male Sprague–Dawley rats (Charles River) were used. The animals were kept on a 12-h light cycle in a room maintained at 22°C and 40%–60% humidity. They were provided a standard diet and tap water ad libitum before and during the experimental period. All animal experiments were approved by the responsible governmental agency (Regierungspräsidium Tübingen).

Radiochemistry

[11]C-DASB was synthesized as described by Wilson et al. (14). Specific activity (SA) was determined at the start of the PET scans and was 88 ± 30 GBq/μmol in the mouse experiments and 114 ± 41 GBq/μmol in the rat experiments. For the dose–response experiments, the SA was adjusted from 0.5 to 180 GBq/μmol in rats and from 0.5 to 116 GBq/μmol in mice. The upper limit of the injection volume was 65 μL in mice and 100 μL in rats. Injected activities, specific activities, injected mass, and injected dose for the multiple-ligand concentration transporter assay are indicated in Table 1.

Anesthesia Protocols

The anesthetics 1.5% isoflurane vaporized in breathing air (21% O_2; 79% N_2) and medetomidine–midazolam for ^{11}C-DASB PET measurements in mice ($n = 4$) were compared. Medetomidine (0.05 mg/kg) and midazolam (5 mg/kg) were dissolved in saline and applied intraperitoneally 20 min before PET data acquisition. For isoflurane and medetomidine–midazolam measurements, the respective SAs were 102 ± 13 and 113 ± 24 GBq/μmol and the respective injected doses were 4.2 ± 0.3 and 3.9 ± 0.8 nmol/kg.

PET Data Acquisition, Reproducibility, and Reliability

The PET procedures and calculation of reproducibility and reliability are described in the supplemental materials (available at http://jnm.snmjournals.org).

Determination of Binding Parameters

Kinetic Modeling Using Simplified Reference Tissue Model. The PET data of all high-SA measurements were analyzed, and the time–activity curves and resulting BP_{ND} obtained using the volume-of-interest modifications were compared.

The thalamus was used as the target tissue because it had the highest uptake, and the different modifications of the cerebellum were used as the reference region in subsequent experiments. To determine BP_{ND}, we used the simplified reference tissue model (Eq. 1) (9):

$$C(t) = R_1 C_r(t) + R_1 \left[k_2' - k_2 \right] C_r(t) \otimes e^{-k_2 t}, \qquad \text{Eq. 1}$$

where $C(t)$ and $C_r(t)$ are regional radioactivity concentration in the target and reference regions, respectively; k_2 is the clearance rate constant from target tissue to plasma; k_2' is the rate constant from reference tissue to plasma; and R_1 is relative radioligand delivery ($R_1 = K_1/K_1'$). The estimated parameters obtained from nonlinear fitting were BP_{ND}, R_1, k_2', and k_2.

Calculation of B_{avail} and appK_D from Competition Experiments. For in vitro measurements under constant conditions, BP is defined as the ratio of receptor density (B_{max}) and the equilibrium dissociation rate constant (K_D). Because the affinity of ligand binding is the inverse of K_D, BP can be equivalently expressed as the product of B_{max} and affinity (Eq. 2).

$$BP = \frac{B_{max}}{K_D} = B_{max} \times \frac{1}{K_D} = B_{max} \times \text{affinity}. \qquad \text{Eq. 2}$$

In in vivo PET, for which conditions depend on many physiologic parameters (body temperature, blood flow, receptor/transporter availability), BP is calculated as the ratio of the available receptor density (B_{avail}) to the apparent equilibrium dissociation rate constant (appK_D).

To calculate B_{avail} and appK_D, the multiple-ligand concentration transporter assay was performed. This approach is derived from in vitro saturation experiments. Rats and mice were injected with increasing concentrations of DASB, which was added to the tracer solution (Table 1).

To calculate the parameters B_{avail} and appK_D, nonlinear regression analysis (Eq. 3) was used as previously described (15–17):

$$\frac{B}{F} = \frac{B_{avail}}{\text{appK}_D + F}, \qquad \text{Eq. 3}$$

where B is the concentration of bound ligand, B_{avail} is the available receptor density in vivo, F is the free radioligand concentration in tissue, and appK_D is the dissociation rate constant under in vivo conditions (16). In PET receptor studies, B and F are calculated from the

TABLE 1
Scan Parameters

Species and SA level	Injected activity (MBq)	SA (GBq/μmol)	Injected mass (μg/kg)	Injected dose (nmol/kg)
Mouse				
High	13.0 ± 0.7	75.2 ± 21.6	2.5 ± 0.3	7.7 ± 2.2
Medium	12.9 ± 0.6	32.3 ± 1.5	11.7 ± 0.2	16.0 ± 0.3
Low	12.5 ± 0.2	5.1 ± 0.2	29.5 ± 0.7	101.2 ± 1.5
Very low	12.5 ± 0.3	0.5 ± 0.01	217.6 ± 2.5	980.5 ± 10.8
Rat				
High	21.5 ± 1.4	126.3 ± 36.4	0.16 ± 0.1	0.6 ± 0.2
Medium	23.1 ± 0.4	65.9 ± 2.5	0.6 ± 0.3	1.1 ± 0.1
Low	22.1 ± 0.3	13.3 ± 5.7	4.4 ± 2.4	3.1 ± 0.1
Very low	22.9 ± 0.4	0.5 ± 0.02	24.4 ± 1.1	26.7 ± 1.1

time–activity curve of the target region (C_{target}) and the reference region (C_{ref}):

$$B = \frac{C_{target} - C_{ref}}{SA} \qquad \text{Eq. 4}$$

$$F = \frac{C_{ref}}{SA - f_{ND}}, \qquad \text{Eq. 5}$$

with f_{ND} being the portion of free tracer in tissue. Because f_{ND} can be determined only by using an arterial input function, BP_{ND} is not corrected for f_{ND}.

K_D can also be defined as the effective dose (ED_{50}). ED_{50} represents the concentration of free ligand that is required to occupy 50% of the transporter sites.

Choice of Correct Reference Region. The cerebellum is a commonly used reference region in human ^{11}C-DASB PET brain studies. Because some serotonergic fibers also project to parts of the cerebellum, we compared 3 possibilities for the use of the cerebellum as a suitable reference region. In both mice and rats, we used, first, the whole cerebellum and, second, the cerebellum with fully saturated binding sites, which was obtained from measurements at a very low SA. In rats, as the third possible reference region we also used the cerebellar cortex, which was indistinguishable from the cerebellar white matter in mice. For this purpose, the volume of interest of the gray matter was adjusted to the entire gray matter of the cerebellum.

Statistical Analysis

To evaluate differences in the calculated binding parameters, we used a paired-sample *t* test with a *P* value of less than 0.05 considered significant. The data are represented as mean $\pm$ SD. Test–retest variability and reliability were evaluated using 1-way ANOVA. To analyze data from the multiple-ligand concentration transporter assay, we used Origin 8.0 (OriginLab) to perform linear and nonlinear regressions.

RESULTS

Determination of Anesthesia Protocol

Representative decay-corrected time–activity curves of the thalamus and cerebellum of 4 mice under isoflurane and medetomidine–midazolam anesthesia are illustrated in Figure 1. Uptake of ^{11}C-DASB (11.8% $\pm$ 1.4%) in the thalamus was almost 2-fold higher under isoflurane than under medetomidine–midazolam (6.9% $\pm$ 0.05%). In addition, the time to peak ^{11}C-DASB uptake was about 210 s under isoflurane and about 900 s under medetomidine–midazolam, whereas the clearance half-life was about 2,700 and 4,500 s, respectively.

Time–Activity Curves and Choice of Reference Region

PET images and the corresponding decay-corrected time–activity curves at different SAs are shown in Figure 2 for one mouse and in Figure 3 for one rat. Thalamic (Fig. 2B) uptake of injected ^{11}C-DASB activity per cubic centimeter was 15% in mice but only 1% in rats (Fig. 3B).

Specific binding in the thalamus (Figs. 2B and 3B) and cerebellum (Figs. 2C, 3C, and 3D) decreased with increasing tracer doses. In rats, the difference for the cerebellum between high and very low SAs was smaller when the cerebellar cortex (Fig. 3D) was used as the reference region than when the whole cerebellum (Fig. 3C) was used. In mice, the cerebellar cortex could not be distinguished from the cerebellar white matter. The time–activity curves for the cerebellar cortex were too noisy for kinetic analysis because of the small size of the mouse brain and of the cerebellum in particular.
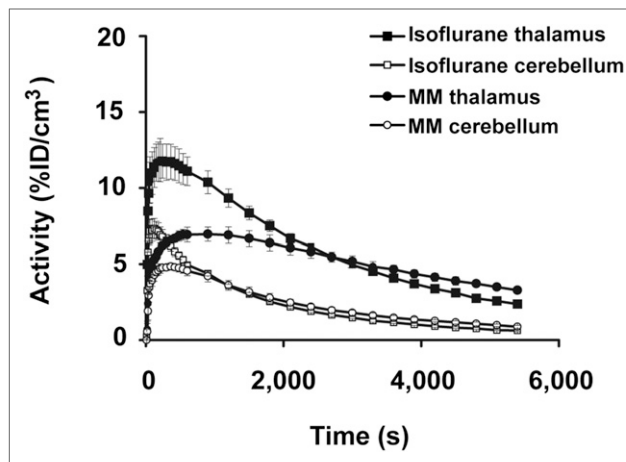

FIGURE 1. Comparison of anesthesia protocols. Time–activity curves of ^{11}C-DASB in thalamus and cerebellum show higher brain uptake under isoflurane anesthesia than under medetomidine–midazolam anesthesia. Time to peak uptake of ^{11}C-DASB was about 210 s under isoflurane and about 900 s under medetomidine–midazolam. %ID = percentage injected dose; MM = medetomidine–midazolam.

Correlation of BP_{ND} Obtained Using Different Reference Regions

Applying the simplified reference tissue model to our PET data using the different reference tissues showed stable fits in both mice (Supplemental Fig. 1A) and rats (Supplemental Fig. 1B).

Linear regression analysis was performed of BP_{ND} calculated using cerebellum with fully saturated binding sites (at a very low SA), whole cerebellum, and cerebellar cortex as the reference regions (Supplemental Fig. 2). In both rats and mice, BP_{ND} calculated from cerebellum with fully saturated binding sites showed very high variability and did not correlate with BP_{ND} calculated from whole cerebellum (Supplemental Figs. 2A and 2B) or cerebellar cortex (Supplemental Fig. 2C). In contrast, in rats, BP_{ND} calculated using whole cerebellum correlated strongly with BP_{ND} calculated using cerebellar cortex (Supplemental Fig. 2D; $R^2 = 0.9$).

When cerebellum with fully saturated binding sites was used as the reference tissue, BP_{ND} was higher and more scattered (mouse, 3.6–6.3; rat, 1.9–3.2) than when whole cerebellum (mouse, 1.5–1.8; rat, 1.4–1.7) or cerebellar cortex (rat, 1.4–1.9) was used.

Test–Retest Experiments

The test–retest data obtained using the whole cerebellum as the reference region in mice and rats, as well as using the cerebellar cortex as the reference region in rats, are summarized in Supplemental Table 1. The test–retest reproducibility for the thalamus using the simplified reference tissue model was 95% for mice and 92% for rats. In regions with lower binding, such as the striatum and hippocampus, reproducibility was only slightly lower: 93% and 90% for mice and 89% and 91% for rats. Reliability was 43% in the thalamus, 14% in the striatum, and 4% in the hippocampus for rats. Reliability could not be determined for the mouse measurements.

Determination of B_{avail} and appK_D

According to the assumptions of a single-binding-site model and using the concentration of the whole cerebellum (mouse) as an estimate of free ligand concentration, calculation of the parameters B_{avail} and appK_D using nonlinear regression analysis did not result in an accurate fit (Fig. 4A). In contrast, in rats, nonlinear regression analysis using the cerebellar cortex as the reference
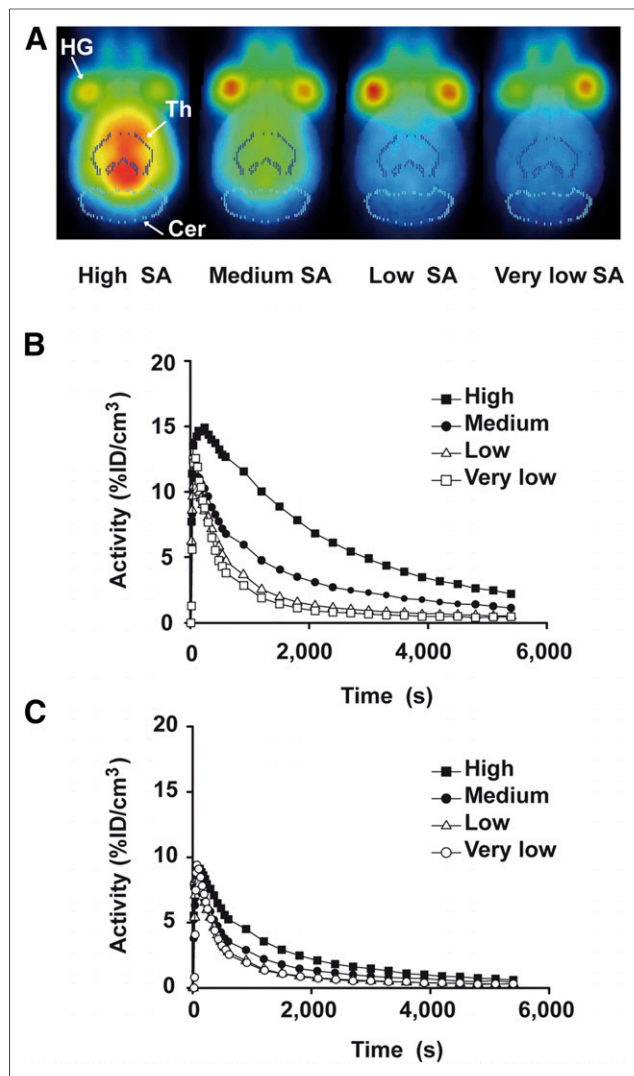
FIGURE 2. ^{11}C-DASB brain uptake in mice. Normalized PET images with decreasing SA in mice (A) and corresponding time–activity curves of thalamus (B) and cerebellum (C). Mouse cerebellum showed displaceable binding of ^{11}C-DASB with decreasing SA (increasing tracer mass). Cer = cerebellum; HG = Harderian gland; %ID = percentage injected dose; Th = thalamus.

region revealed a B_{avail} and $appK_D$ of 3.9 ± 0.7 pmol/mL and 2.2 ± 0.4 nM, respectively (Fig. 4B). The results for the different reference tissues are summarized in Supplemental Table 2.

To calculate the ED_{50}, the BP_{ND} was plotted as a function of injected dose in nmol/kg (Supplemental Fig. 3) and Equation 3 was applied. The highest BP_{ND} ranged from 1.5 to 1.8 in mice and from 1.4 to 1.9 in rats. The ED_{50} could not be calculated for the mouse data because of the inappropriate regression result (Supplemental Fig. 3A). In rats, the ED_{50} was 12.0 ± 2.6 nmol/kg (Supplemental Fig. 3B).

DISCUSSION

This study was, to our knowledge, the first in vivo evaluation of ^{11}C-DASB for quantitative SERT imaging in mice. Before transgenic animal models of human diseases can be used in PET brain studies, careful evaluation of the radioligand and the PET methodology for in vivo quantification is needed.

The choice of anesthesia is important in small-animal PET experiments because it can have a considerable impact on receptor availability, tracer uptake, cerebral blood flow, cerebral blood volume, and brain metabolism (18,19). To date, little has been known on whether PET findings using the serotonin reuptake inhibitor ^{11}C-DASB are affected by different types of anesthesia. In one study, Stehouwer et al. performed PET measurements with a newly devel-

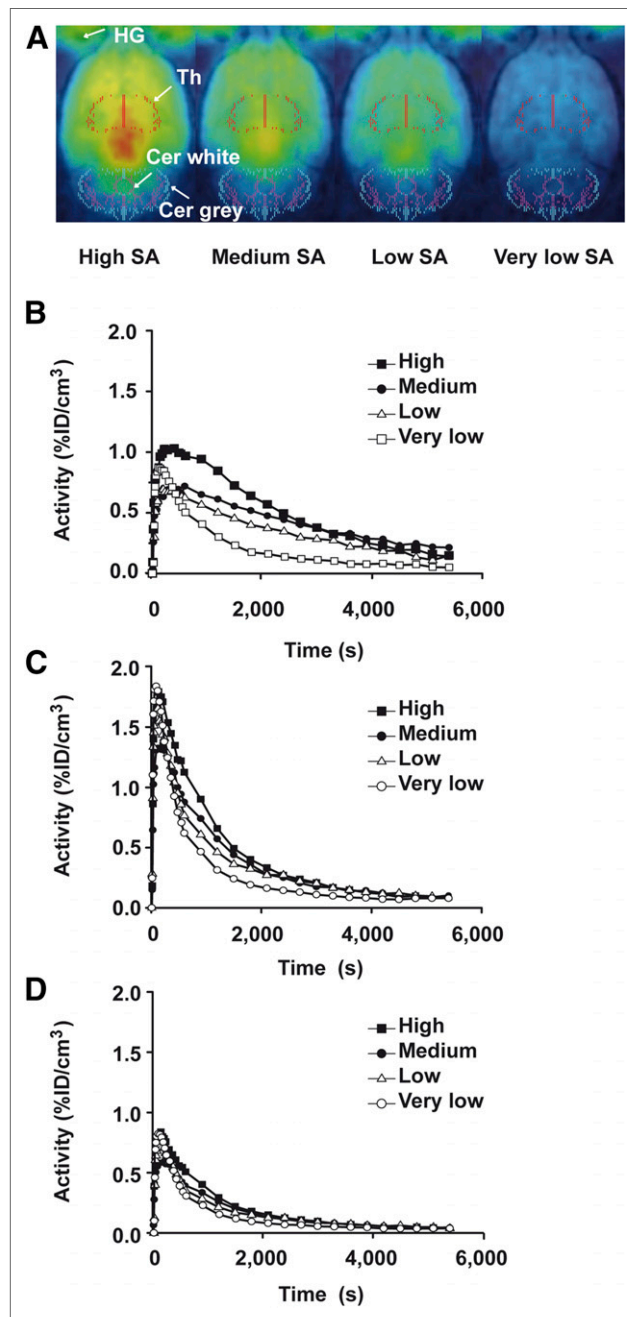FIGURE 3. ^{11}C-DASB brain uptake in rats. Normalized PET images with decreasing SA in rats (A) and corresponding time–activity curves of thalamus (B) and cerebellum (C). The rat cerebellum showed displaceable binding of ^{11}C-DASB with decreasing SA (increasing tracer mass). Using the cerebellar cortex as reference region, displaceable binding was considerably reduced (D). Cer = cerebellum; HG = Harderian gland; %ID = percentage injected dose; Th = thalamus.
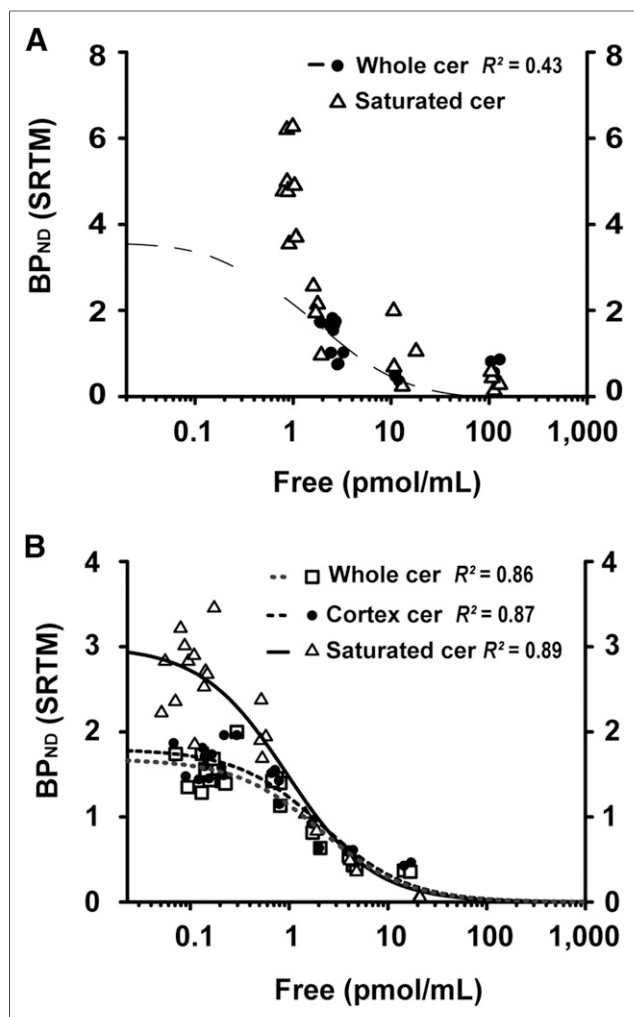
FIGURE 4. Calculation of B_{avail} and $appK_D$ of ^{11}C-DASB in mice and rats. For determination of binding parameters B_{avail} and $appK_D$, BP_{ND} was plotted against free fraction of ^{11}C-DASB and analyzed using nonlinear regression analysis. For mouse brain data, no appropriate fit could be obtained (A). In rats, B_{avail} and $appK_D$ obtained using the cerebellar cortex as reference tissue were 3.9 ± 0.6 pmol/mL and 2.2 ± 0.4 nM, respectively (B). B also illustrates the impact of specific binding in the reference tissue on BP_{ND}. The cerebellum with saturated binding sites produced higher but more scattered BP_{ND} estimates than the whole cerebellum or cerebellar cortex. cer = cerebellum; SRTM = simplified reference tissue model.

oped SERT radioligand on conscious, isoflurane-anesthetized monkeys and demonstrated that uptake was not influenced by isoflurane (20). However, experiments on rats and mice that are awake are usually performed under conditions of restraint, resulting in stress on the animals and therefore altered binding parameters. Our data showed that when measuring ^{11}C-DASB in mice, the use of medetomidine–midazolam anesthesia resulted in lower brain tracer uptake, a longer time to peak, and longer half-life clearance than with isoflurane anesthesia. This finding may be related to the independent impacts of the two anesthetics on blood pressure (21,22). Because isoflurane is easier to adjust and maintain individually, it is a convenient anesthesia for PET scanning procedures and was applied in all the following experiments.

Uptake of ^{11}C-DASB in the brain was 15-fold lower in rats than in mice because of the 15-fold higher brain-to-body weight ratio of

rats. Specific binding of ^{11}C-DASB was observed in both rats and mice, with the highest uptake being in the thalamus, hippocampus, and striatum, in line with in vivo PET studies on humans and rats (23,24). Displaceable binding was also observed in the cerebellum, which is a commonly used reference region in PET brain studies because of the assumption that it has a negligible number of binding sites (23,24). Nevertheless, serotonin fibers are known to project from the raphe nuclei into the cerebellum (25,26). Although the cerebellar white and gray matter showed the same distribution of SERT binding sites, a suitable reference region should have free and nonspecific binding properties similar to those of the region with specific binding. These binding properties are highly dependent on the proteins that bind the radioligand nonspecifically. Therefore, Parsey et al. have suggested that the cerebellar cortex is the best available reference region for ^{11}C-DASB PET studies (26). This is in line with our findings, which showed the lowest specific binding and comparable unspecific binding when the cerebellar cortex was used as the reference region in rats, rather than the whole cerebellum. In mice, we were unable to accurately distinguish between cerebellar gray and white matter because of the small size of the mouse cerebellum. In addition, spillover from adjacent brain regions (e.g., from the midbrain and fourth ventricle) can lead to overestimation of the time–activity curve values and hence underestimation of BP_{ND}. Furthermore, if competition binding experiments with increasing concentrations of the cold ligand are performed to calculate B_{avail} and $appK_D$, specific binding in the cerebellum will differ for each concentration and will therefore alter the cerebellar time–activity curve, leading to errors in the estimated parameters.

We used the cerebellar cortex as reference region for rats. However, because this approach was not feasible in mice, we used the whole cerebellum as reference tissue, taking the specific binding in the reference region into account and remaining aware of the underestimation of the determined BP_{ND}.

In clinical human PET studies, an arterial input function is often used to calculate binding parameters from individual kinetic parameters if no adequate reference region is available (24,27). However, in small laboratory animals, an arterial input function is invasive and difficult to generate via catheterization of arterial vessels, especially in longitudinal experiments, because the animals have to be sacrificed after the PET measurement. In a clinical human PET study, Frankle et al. compared the results obtained for ^{11}C-DASB using an arterial input function and the simplified reference tissue model and reported that both methods resulted in similar values across all regions (24), confirming that arterial blood sampling is not mandatory for the analysis of human ^{11}C-DASB PET data.

The reference tissue model described by Watabe et al. is a kinetic modeling approach that includes and describes specific binding in the reference tissue (28). This model describes a single tissue compartment for the target tissue and two tissue compartments for the reference tissue, assuming a certain amount of specific binding in the reference tissue. However, a disadvantage of this full-reference-tissue approach is its complexity, which is due to the quantity of undefined parameters for the reference region. Therefore, the parameters need to be estimated from a receptor-rich target region and can then be fixed to constant values. However, using simulations, Millet et al. found few improvements when using this method compared with the simplified reference tissue model (29).

Another approach to address specific binding in the reference region is the use of the cerebellum with fully saturated binding sites. With this approach, an additional PET scan is required to fully saturate the cerebellum. In our experiments, the BP_{ND} using

this approach showed higher intersubject variability than when obtained using the whole cerebellum or cerebellar cortex as the reference tissue. This discrepancy may relate to the use of target and reference tissues from two different scans. Additionally, the time–activity curves from the cerebellum with fully saturated binding sites were much noisier, leading to greater variability in estimated BP_{ND}.

In both mice and rats, we found good reproducibility for the calculated binding parameters in a SERT-rich region (thalamus, 95% and 92%, respectively) and only slightly lower reproducibility in a region of moderate SERT binding (striatum, 93% and 89%, respectively). These findings agree closely with PET data from cats (thalamus, 92%; striatum, 88%) and are only slightly lower than data from humans (thalamus, 89.5%; striatum, 93%) (24,30,31). The reliability of the rat measurements was higher in the thalamus (43%) than in the striatum (14%), as is in line with the literature (24). However, the reliability of mouse test–retest experiments could not be calculated because the mean sum square between subjects was smaller than the mean sum square within subjects.

In tracer-binding experiments, quantification of receptor or transporter concentrations and radioligand affinity is generally performed ex vivo with long-lived isotopes (32,33). These studies are performed under controlled and constant (buffer, pH, temperature) conditions. Compared with the in vitro situation, membrane receptors and transporters and in particular the 5-HTergic system, which contributes to numerous essential brain networks such as those related to circadian rhythm and anxiety, show highly dynamic behavior, including internalization and externalization as well as conformational changes from high- to low-affinity states (34). In addition, the BP_{ND} calculated from a single-injection PET experiment reflects both B_{avail} and $appK_D$ (35). Therefore, in vivo evaluation of SERT density and radioligand affinity will considerably improve the interpretation of PET results in many experiments. Here, we provide the first test, to our knowledge, of the feasibility of using the multiple-ligand concentration transporter assay to determine B_{avail} and $appK_D$ for ^{11}C-DASB in mice and rats under in vivo conditions. In rats, with the cerebellar cortex as the reference region, B_{avail} (3.9 ± 0.7 pmol/mL) was comparable to B_{max} obtained in an ex vivo binding study by Elfving et al. using rat brain tissue homogenates (3.0 ± 0.1 pmol/mL) (36). We obtained higher $appK_D$ values (2.2 ± 0.4 nM) than the K_D values reported by Elfving et al. (0.34 nM), as might be explained by the different experimental setups of the in vivo and ex vivo binding experiments. The calculated ED_{50} was 12.0 ± 2.6 nmol/kg, which was lower than that found in an ex vivo study on rats (51 nmol/kg) (23). The rat brains were etched and fragmented into different brain regions and measured in a γ-counting device. This could explain the differences from our data; γ-counting measurements result in higher activity outcomes than in vivo PET measurements because of the partial-volume effects in PET experiments (37).

In mice, nonlinear regression analysis did not lead to accurate fits for the determination of B_{avail}, $appK_D$, and ED_{50}. This can be explained by the fact that in our experiments, a plateau could not be reached for BP_{ND} with the highest obtainable SA (Fig. 4 and Supplemental Fig. 3). The lower brain-to-body weight ratio of the mice resulted in a 15-fold higher tracer uptake and a 13- to 15-fold higher injected mass in the mice (2.5 ± 0.3 μg/kg) than in the rats (0.16 ± 0.1 μg/kg).

Additionally, mouse BP_{ND} was higher at a very low SA than at a low SA. This could be due to an underestimation of BP_{ND} at high-to-low SAs because of specific binding in the cerebellum if the binding sites of the reference region are not totally saturated, as well as to differences in nondisplaceable binding between the target and reference regions.

Therefore, PET measurements in mice should be performed at a significantly lower injected activity to obtain lower transporter occupancy or produce ^{11}C-DASB at higher SAs; this requires a PET scanner with high detection sensitivity.

CONCLUSION

Our study showed that, compared with medetomidine–midazolam, isoflurane resulted in a higher tracer uptake and was more easily applied for quantitative in vivo PET measurements in the brains of small laboratory animals. Further, we demonstrated that the cerebellar cortex is an accurate reference region for kinetic modeling in rats but not in mice, because of the small size of the cerebellum in mice. The calculated reproducibility for mice and rats was more than 90% and was comparable to in vivo PET studies on humans. However, when the parameters B_{avail}, $appK_D$, and ED_{50} were calculated, only the rat measurements resulted in good-quality fits. It remains difficult to estimate quantitative parameters accurately from mouse measurements because of the high injected tracer mass and underestimation of binding parameters due to high displaceable binding in the reference region. Higher-SA DASB production is required to achieve a sufficiently low injected mass while maintaining a signal that is sufficient for reliable measurements of quantitative parameters in mouse imaging.

DISCLOSURE

REFERENCES

1. Eskow KL, Dupre KB, Barnum CJ, Dickinson SO, Park JY, Bishop C. The role of the dorsal raphe nucleus in the development, expression, and treatment of L-dopa-induced dyskinesia in hemiparkinsonian rats. *Synapse.* 2009;63:610–620.
2. Hariri AR, Holmes A. Genetics of emotional regulation: the role of the serotonin transporter in neural function. *Trends Cogn Sci.* 2006;10:182–191.
3. Filip M, Frankowska M, Zaniewska M, Gołda A, Przegaliński E. The serotonergic system and its role in cocaine addiction. *Pharmacol Rep.* 2005;57:685–700.
4. Houle S, Ginovart N, Hussey D, Meyer JH, Wilson AA. Imaging the serotonin transporter with positron emission tomography: initial human studies with [^{11}C]DAPP and [^{11}C]DASB. *Eur J Nucl Med.* 2000;27:1719–1722.
5. Murthy NV, Selvaraj S, Cowen PJ, et al. Serotonin transporter polymorphisms (SLC6A4 insertion/deletion and rs25531) do not affect the availability of 5-HTT to [^{11}C] DASB binding in the living human brain. *Neuroimage.* 2010;52:50–54.
6. Wehrl HF, Hossain M, Lankes K, et al. Simultaneous PET-MRI reveals brain function in activated and resting state on metabolic, hemodynamic and multiple temporal scales. *Nat Med.* 2013;19:1184–1189.
7. Hume SP, Jones T. Positron emission tomography (PET) methodology for small animals and its application in radiopharmaceutical preclinical investigation. *Nucl Med Biol.* 1998;25:729–732.
8. Laruelle M, Slifstein M, Huang Y. Positron emission tomography: imaging and quantification of neurotransporter availability. *Methods.* 2002;27:287–299.
9. Lammertsma AA, Hume SP. Simplified reference tissue model for PET receptor studies. *Neuroimage.* 1996;4:153–158.
10. Hassoun W Le Cavorsin M, Ginovart N, et al. PET study of the [^{11}C]raclopride binding in the striatum of the awake cat: effects of anaesthetics and role of cerebral blood flow. *Eur J Nucl Med Mol Imaging.* 2003;30:141–148.

11. Alstrup AK, Landau AM, Holden JE, et al. Effects of anesthesia and species on the uptake or binding of radioligands in vivo in the Gottingen minipig. *BioMed Res Int.* 2013;2013:808713.

12. Martin DC, Adams RJ, Aronstam RS. The influence of isoflurane on the synaptic activity of 5-hydroxytryptamine. *Neurochem Res.* 1990;15:969–973.

13. Holden JE, Jivan S, Ruth TJ, Doudet DJ. In vivo receptor assay with multiple ligand concentrations: an equilibrium approach. *J Cereb Blood Flow Metab.* 2002;22:1132–1141.

14. Wilson AA, Jivan S, Ruth TJ, Doudet DJ. Novel radiotracers for imaging the serotonin transporter by positron emission tomography: synthesis, radiosynthesis, and in vitro and ex vivo evaluation of ^{11}C-labeled 2-(phenylthio)araalkylamines. *J Med Chem.* 2000;43:3103–3110.

15. Fischer K, Sossi V, Schmid A, et al. Noninvasive nuclear imaging enables the in vivo quantification of striatal dopamine receptor expression and raclopride affinity in mice. *J Nucl Med.* 2011;52:1133–1141.

16. Hume SP, Opacka-Juffry J, Myers R, et al. Effect of L-dopa and 6-hydroxydopamine lesioning on [^{11}C]raclopride binding in rat striatum, quantified using PET. *Synapse.* 1995;21:45–53.

17. Scatchard G. The attractions of proteins for small molecules and ions. *Ann N Y Acad Sci.* 1949;1949:660–672.

18. Alstrup AK, Smith DF. Anaesthesia for positron emission tomography scanning of animal brains. *Lab Anim.* 2013;47:12–18.

19. Fuchs K, Kukuk D, Mahling M, et al. Impact of anesthetics on 3′-[^{18}F]fluoro-3′-deoxythymidine ([^{18}F]FLT) uptake in animal models of cancer and inflammation. *Mol Imaging.* 2013;12:277–287.

20. Stehouwer JS, Jarkas N, Zeng F, et al. Synthesis, radiosynthesis, and biological evaluation of fluorine-18-labeled 2beta-carbo(fluoroalkoxy)-3beta-(3′-((Z)-2-haloethenyl)phenyl)nortropanes: candidate radioligands for in vivo imaging of the serotonin transporter with positron emission tomography. *J Med Chem.* 2008;51:7788–7799.

21. Sinclair MD. A review of the physiological effects of alpha2-agonists related to the clinical use of medetomidine in small animal practice. *Can Vet J.* 2003;44:885–897.

22. Homi J, Konchigeri HN, Eckenhoff JE, Linde HW. A new anesthetic agent: Forane—preliminary observations in man. *Anesth Analg.* 1972;51:439–447.

23. Wilson AA, Ginovart N, Hussey D, Meyer J, Houle S. In vitro and in vivo characterisation of [^{11}C]-DASB: a probe for in vivo measurements of the serotonin transporter by positron emission tomography. *Nucl Med Biol.* 2002;29:509–515.

24. Frankle WG, et al. Estimation of serotonin transporter parameters with ^{11}C-DASB in healthy humans: reproducibility and comparison of methods. *J Nucl Med.* 2006;47:815–826.

25. Bishop GA, Ho RH. The distribution and origin of serotonin immunoreactivity in the rat cerebellum. *Brain Res.* 1985;331:195–207.

26. Parsey RV, Slifstein M, Gunn RN, et al. Acute occupancy of brain serotonin transporter by sertraline as measured by [^{11}C]DASB and positron emission tomography. *Biol Psychiatry.* 2006;59:821–828.

27. Ogden RT, Ojha A, Erlandsson K, Oquendo MA, Mann JJ, Parsey RV. In vivo quantification of serotonin transporters using [^{11}C]DASB and positron emission tomography in humans: modeling considerations. *J Cereb Blood Flow Metab.* 2007;27:205–217.

28. Watabe H, Carson RE, Iida H. The reference tissue model: three compartments for the reference region. *NeuroImage.* 2000;11(part 2):S12.

29. Millet P, Graf C, Buck A, Walder B, Ibáñez V. Evaluation of the reference tissue models for PET and SPECT benzodiazepine binding parameters. *Neuroimage.* 2002;17:928–942.

30. Ginovart N, Wilson AA, Meyer JH, Hussey D, Houle S. [^{11}C]-DASB, a tool for in vivo measurement of SSRI-induced occupancy of the serotonin transporter: PET characterization and evaluation in cats. *Synapse.* 2003;47:123–133.

31. Kim JS, Ichise M, Sangare J, Innis RB. PET imaging of serotonin transporters with [^{11}C]DASB: test-retest reproducibility using a multilinear reference tissue parametric imaging method. *J Nucl Med.* 2006;47:208–214.

32. Marjamäki P, Zessin J, Eskola O, et al. S-[^{18}F]fluoromethyl-(+)-McN5652, a PET tracer for the serotonin transporter: evaluation in rats. *Synapse.* 2003;47:45–53.

33. Palner M, Underwood MD, Kumar DJ. Ex vivo evaluation of the serotonin 1A receptor partial agonist [^{3}H]CUMI-101 in awake rats. *Synapse.* 2011;65:715–723.

34. Meneses A, Liy-Salmeron G. Serotonin and emotion, learning and memory. *Rev Neurosci.* 2012;23:543–553.

35. Innis RB, Cunningham VJ, Delforge J, et al. Consensus nomenclature for in vivo imaging of reversibly binding radioligands. *J Cereb Blood Flow Metab.* 2007;27:1533–1539.

36. Elfving B, Madsen J, Knudsen GM. Neuroimaging of the serotonin reuptake site requires high-affinity ligands. *Synapse.* 2007;61:882–888.

37. Elsässer-Beile U, Reischl G, Wiehr S, et al. PET imaging of prostate cancer xenografts with a highly specific antibody against the prostate-specific membrane antigen. *J Nucl Med.* 2009;50:606–611.